JOURNAL OF SPACECRAFT AND ROCKETS
Vol. 35, No. 6, November–December 1998

Aerodynamic Heating Measurement on Afterbody of Hypersonic Flight Experiment

Keisuke Fujii* and Yasutoshi Inoue†
National Aerospace Laboratory, Chofu, Tokyo 182-8522, Japan

Measured aerodynamic heating over the ceramic tile region of the Hypersonic Flight Experiment vehicle was obtained on Feb. 12, 1996. Measurements obtained on this lifting hypersonic vehicle during its suborbital flight at velocities up to 3.88 km/s have been compared with heating correlations. Results of the comparisons of obtained measurements to predictions show good agreement for local-to-stagnation Stanton number ratio. Flight measurements also showed that boundary-layer transition occurred on the windward side and that the position of transition moved forward to a location aft of the nose equal to about 30% of the total vehicle length. Local flow conditions, where transition was observed, are evaluated with a criterion for attachment line transition of a yawed cylinder, and the results show fair agreement providing that the surface roughness effect is taken into account. During flight, relaminarization followed transition along the fore part of the vehicle. This relaminarization is surmised to be due to decreasing Reynolds number along the flight path when the effect of variable entropy, caused by nose bluntness, is accounted for.

Nomenclature

C = specific heat, J/kg K
h = enthalpy, J/kg
k = boundary-layer edge velocity gradient normal to axis, dv_e/dy, 1/s
L = vehicle length, 4 m
M = Mach number
N = reciprocal exponent in velocity profile power law in turbulent boundary layer
Pr = Prandtl number of air, 0.72
q = heating rate, W/m^2
$\bar{R}$ = Reynolds number based on a characteristic length η
Re = Reynolds number
St = Stanton number
$\overline{St}$ = Stanton number ratio, St/St_0
T = temperature, °C
t = time after separation from J-1 launcher, s
u = velocity along vehicle axis (x component), m/s
V = freestream velocity
v = y component of velocity, m/s
x, y = coordinates; see Fig. 4
α = angle of attack, deg
Δs = effective roughness height of gaps and steps
ε_{in} = absorptivity of glass coating for Xe lamp
ε_{out} = emissivity of glass coating
η = characteristic length [Eq. (2)], m
κ = heat conductivity, W/m K
μ = viscosity, kg/m s
ν = kinematic viscosity, m^2/s
ρ = density, kg/m^3

Subscripts

coat = value of glass coating
e = condition at the edge of boundary layer
tile = value of ceramic tile
w = wall condition
0 = stagnation condition
∞ = freestream value

Superscript

$*$ = reference condition determined from temperature T^* equal to $0.3T_e + 0.1T_w + 0.6T_0$

Received Feb. 12, 1998; revision received July 6, 1998; accepted for publication July 20, 1998.

*Researcher, Aerodynamics Division. Member AIAA.
†Director, Aerodynamics Division. Senior Member AIAA.

Introduction

SEVERAL methods have been developed for estimating the aerodynamic heating rate and predicting the occurrence of boundary-layer transition on a hypersonic flight vehicle. In fact, several engineering methods are currently being used in designing HOPE-X, Japan's reusable, winged, re-entry experiment vehicle planned by the National Aerospace Laboratory (NAL) and National Space Development Agency of Japan. The axisymmetric analog technique reported by Zoby et al.[1] and DeJarnette and Davis[2] shows good correlation with Space Shuttle heat transfer data and is useful in calculating boundary-layer thickness and local flow conditions at the edge of the boundary layer, taking into consideration the effect of variable entropy on the windward side.

To predict boundary-layer transition in designing the Space Shuttle, a ratio of momentum thickness Reynolds number and Mach number at the edge of boundary layer (Re_θ/M_e) was used, whereas a Reynolds number based on effective roughness height was used to determine the criteria for placement of gaps and steps among Space Shuttle tiles.[3] It appears, however, that the critical value for transition of the parameter Re_θ/M_e is dependent on many other parameters such as vehicle configuration, wall temperature, and trajectory. Moreover, to accurately calculate momentum thickness, an accurate velocity field in which variable entropy effects are taken into account is necessary, e.g., use of an Euler code. Here, to avoid such uncertainties and difficulties in the calculation, a criterion for attachment line transition of a yawed cylinder is applied to a hypersonic flight vehicle. The applied criterion has the same tendency in Mach number at the boundary-layer edge, M_e, as $Re_\theta/M_e = \text{const}$ in high M_e, as noted by Poll.[4]

In the analysis of boundary-layer transition, the effect of roughness must be taken into account.[4] Based on various flight results, Poll also showed that the critical roughness height for attachment line transition exists at $0.8 < \Delta s/\eta < 1.6$ for incompressible flow, whereas in hypersonic experiments, Murakami et al.[5] reported that under their test conditions critical roughness height is at $0.2 < \Delta s/\eta^* < 1.4$, with the corresponding freestream Mach number ranging from 5.0 to 6.9 and sweep angle from 30 to 60 deg.

For validation purposes, it is important that results from the preceding methods be compared with those from flight tests in the hypersonic region. The Hypersonic Flight Experiment (HYFLEX) was designed to provide hypersonic flight data on aerodynamic and

aerothermodynamic characteristics and successfully did so in February 1996.[6–9]

In this paper, measured aerodynamic heating rates over the ceramic tile region of the HYFLEX vehicle are compared with both wind-tunnel results and calculations using the axisymmetric analog approach. For these comparisons, heating results are expressed in terms of the local to stagnation Stanton number ratio. In addition, conditions for which boundary-layer transition and relaminarization occurred in flight are compared with Poll's criterion.[4]

Flight Test

HYFLEX was separated from the J-1 launcher at an altitude of 107 km and a relative velocity of 3.88 km/s, where the dynamic pressure is too small to provide enough aerodynamic lift to sustain the vehicle weight. Consequently, the vehicle dived, producing a flight path in the altitude–velocity plane that had an undershoot trajectory rather than an equilibrium glide path (Fig. 1). The maneuver was achieved by maintaining an angle of attack at 49 deg, as shown in Fig. 2. During this maneuver, the freestream Reynolds number, based on the vehicle length, varied from about 2×10^2 to 3×10^6 (Fig. 3). Subsequently, the vehicle's angle of attack was reduced to about 30 deg and then kept at this attitude up to $t = 300$ s. (In this paper, time always originates at vehicle separation.) From the viewpoint of freestream Reynolds number, the undershoot from equilibrium glide path resulted in a unique nearly constant Reynolds number flight path, as shown in Fig. 3.

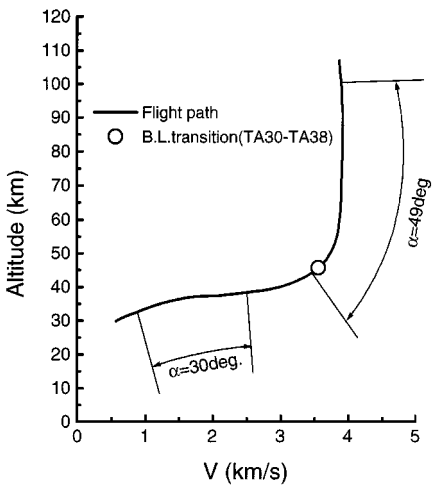

Fig. 1 HYFLEX altitude and velocity history.

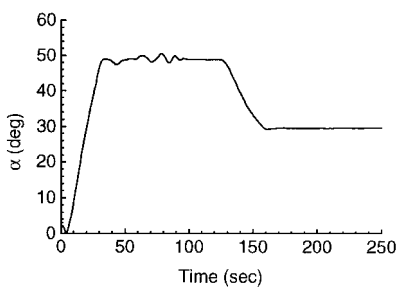

Fig. 2 HYFLEX angle-of-attack history along flight path.

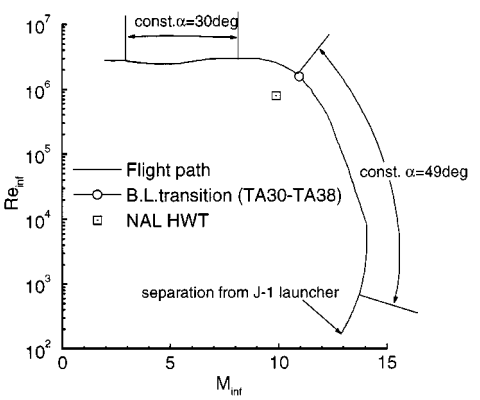

Fig. 3 Freestream Reynolds number vs Mach number along HYFLEX flight path.

Locations of HYFLEX sensors (indicated by TA prefix) for aerodynamic heating measurements are shown in Fig. 4. There were 22 sensors, 8 in the carbon/carbon region, 11 in the ceramic tile region, and 3 in the flexible insulation region. Measured aerodynamic heating rates near the windward centerline are presented for TA21, TA30, TA33, TA35, and TA38.

Sensor and Its Thermal Model

A suitable thermal model is needed to reduce the heat transfer rate from the surface temperature history of the ceramic tiles. However, in measuring or estimating the value of each associated thermal property to allow for model construction, too many sources of error exist that are difficult to accurately estimate, e.g., thermal contact resistance, heat capacity of ceramic cement around a thermocouple, and variations in thermal properties between ceramic tiles. Accordingly, to account for such factors, calibration tests were used to determine parameters that allow the thermal model to fit measured temperature and heat rate data.

Figure 5 shows the simple structure of a sensor, which consists of a cylinder-shaped ceramic tile (diameter 50 mm and length 25 mm) containing three bare thermocouples. The surface thermocouple is situated adjacent to a 0.3-mm-thick glass coating, whereas the second and third thermocouples are located 12 and 25 mm from the surface as indicated.

Prior to the HYFLEX flight, calibration tests were conducted at the Japan Ultra-High Temperature Materials Research Center. A 30-kW Xe-lamp heater was used under several combinations of ambient pressure and heating rate/time. The lamp heating rate was measured separately with Gardon-type heat flux transducers to verify repeatability and time dependency of the lamp heating rate.

Parameters were determined assuming two-dimensional heat conduction, taking temperature dependencies of emissivity and thermal properties into account. With the heating rate from the lamp known, the following four parameters were determined so that the temperature history at the thermocouples showed agreement with measurements in a least-squares sense: 1) ρC_{coat}, heat capacity of SiC coating (effect of thickness of coating); 2) κ_{tile}, conductivity of ceramic tile; 3) ρC_{tile}, heat capacity of ceramic tile; and 4) $\varepsilon_{\text{in}}/\varepsilon_{\text{out}}$, ratio of absorptivity of tile for the light from the Xe lamp to its emissivity.

Although the thickness of the coating is only about 0.3 mm, due to its substantially higher heat capacity in comparison with that of the ceramic tile, its effect on the thermal model cannot be neglected, especially when constant heating is not expected, as is the case for the HYFLEX flight (Fig. 6). In determining parameters dependent on temperature, their dependencies are assumed to be identical to measured nominal values, and only the magnitudes are determined.

A validation test of the total thermal model is carried out using the determined parameters and recalculating the heat rate in which the measured temperature is taken as a boundary condition. A comparison between incident heating rate and the recalculated results is shown in Fig. 7, where there is good agreement except for initial heating, where the model shows higher values. Table 1 shows the nominal properties, and Table 2 summarizes the ratios of the determined to the nominal values for each parameter. Because the sensors were manufactured by two companies (Kawasaki Heavy Industries and Fuji Heavy Industries), their characteristics were slightly different, although the parameters were similarly determined.

Flight-Test Results

Use of the thermal model allows the heating rate to be deduced using measured surface temperature history as the boundary condition. To account for heat conductivity of a ceramic tile, which is dependent not only on temperature but also on internal pressure, we assume that the tile's internal pressure is uniformly equal to the modified Newtonian surface pressure.

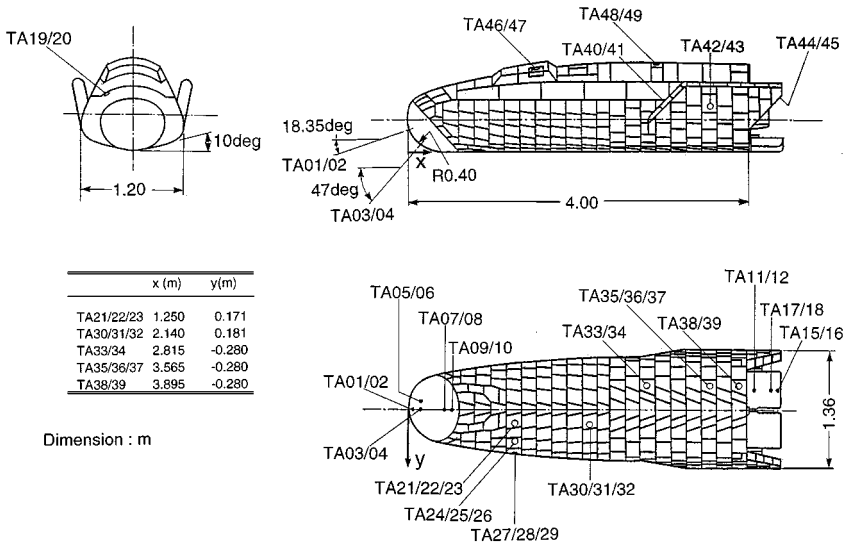

Fig. 4 HYFLEX sensor locations for aerodynamic heating measurement.

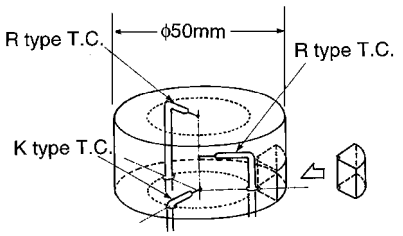

Fig. 5 Structure of HYFLEX ceramic tile sensor.

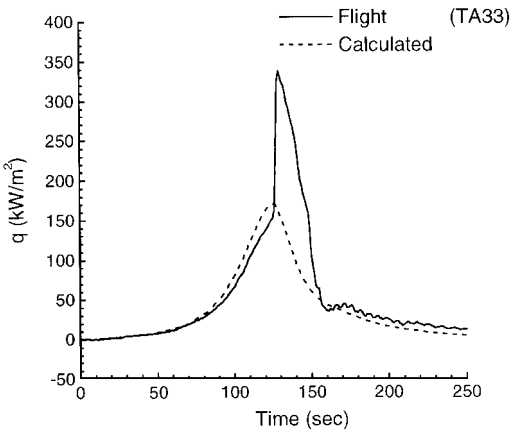

Fig. 6 Measured heating rate at TA33 position.

Data are presented using Stanton number ratio to represent aerodynamic heating, defined as

$$\overline{St} = \frac{St}{St_0}, \qquad St = \frac{q}{\rho_\infty u_\infty (h_0 - h_w)}$$

where St_0 is the value of the Stanton number at the stagnation point determined from the following formula[10]:

$$\frac{q_0}{h_0 - h_w} = 0.763 Pr^{-0.6} \sqrt{\rho_e \mu_e \frac{\mathrm{d}u_e}{\mathrm{d}x}} \qquad (1)$$

Figure 8 presents the inferred Stanton number measured at five locations for the vehicle's windward side as a function of time. While the vehicle was at a nominal angle of attack of 49 deg, the Stanton number ratios decreased gradually with increasing time until an abrupt increase in heating occurred, depending on surface location, between 126 and 136 s. Just before the vehicle achieved a nominal angle of attack of 30 deg, values for three of the sensors (TA21, TA30, and TA33) experienced an abrupt decrease in heating at 148 s.

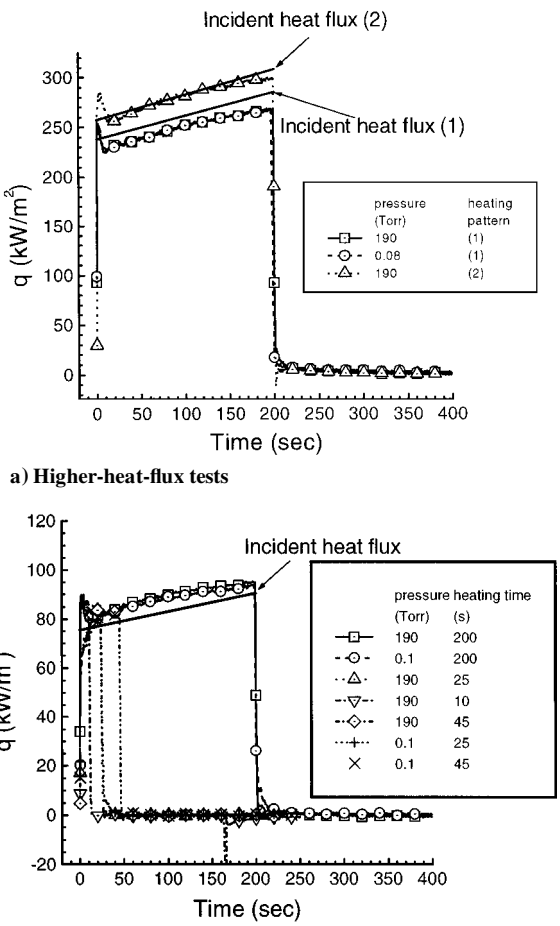

Fig. 7 Recalculated and incident heat flux in lamp heating tests.

This abrupt change in heating is believed to be caused by boundary-layer transition and subsequent relaminarization.

To confirm the occurrence of transition and relaminarization, reference heating rates along the windward centerline were calculated using the axisymmetric analog method[1] in which the entropy at the edge of the boundary layer is assumed to have a constant value just behind the normal shock and N, the reciprocal exponent in the velocity profile power law in the turbulent boundary layer, is also assumed to have a constant value of 7, i.e., $\frac{1}{7}$th power law. The velocity field at the surface and the associated metric coefficient were calculated using the earlier described methods.[2,11] Reference heating rates are

Table 1 Nominal thermal properties used in the model

Parameter	Temperature, °C 25	250	500	750	1000	1200
			Glass coating			
ρ, kg/m^3	3320	3320	3320	3320	3320	3320
C, J/kg K	916	1011	1116	1222	1327	1411
κ, W/m K	2.17	2.17	2.17	2.17	2.17	2.17
			Tile			
ρ, kg/m^3	193.6	193.6	193.6	193.6	193.6	193.6
C, J/kg K[a]	883	1147	1260	1317	1333	1343
C, J/kg K[b]	749	992	1118	1197	1242	1278
κ, W/m K						
0.1 torr	0.029	0.051	0.076	0.102	0.127	0.147
190 torr	0.049	0.071	0.093	0.128	0.168	0.197

[a]Fuji Heavy Industries tiles. [b]Kawasaki Heavy Industries tiles.

Table 2 Determined thermal model parameters for ceramic tiles

Parameter	Fuji Heavy Industries tiles 0.1 torr	190 torr	Kawasaki Heavy Industries tiles 0.1 torr	190 torr
ρC_{coat}	0.830	0.830	1.083	1.083
κ_{tile}				
<750°C	1.726	1.883	1.013	1.152
>1000°C	1.781	2.432	1.407	1.637
ρC_{tile}	1.615	1.615	1.408	1.408
$\varepsilon_{in}/\varepsilon_{out}$	1.002	1.002	0.930	0.930

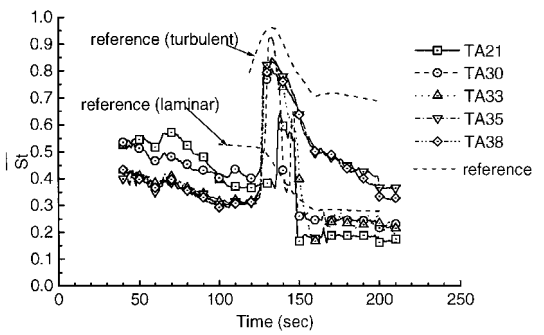

Fig. 8 Measured Stanton number ratios along windward side of HYFLEX.

helpful in that they infer whether the boundary layer is laminar or turbulent. On the other hand, the reference values are expected to be rather different from those measured because 1) the sensor locations on HYFLEX are off centerline and 2) constant entropy is assumed to exist along the streamline such that the estimated heating rate should show a nearly constant distribution. Figure 8 shows the heating rates of the laminar and turbulent boundary layer at the centerline, where the abrupt increase in Stanton number ratio can be seen to be due to boundary-layer transition, whereas the ensuing decrease of TA21, TA30, and TA33 is caused by relaminarization. For TA35 and TA38, however, the boundary layer still appears to be turbulent, with heating rates being higher than the reference laminar value. Why the heating rate at $\alpha = 30$ deg for TA35 and TA38 decreases with time remains unclear.

Wind-Tunnel Test

For postflight analysis purposes, wind-tunnel tests were conducted in the NAL hypersonic wind tunnel to obtain aerothermodynamic data of the laminar boundary layer at corresponding positions. In the tests, $M_\infty = 10$ and $Re_\infty = 0.8 \times 10^6$, based on a model length of 400 mm (Fig. 3). As the freestream Reynolds number is small, the boundary layer at the windward surface is always laminar.

The wind-tunnel model was made of stainless steel (SUS303), and heating rates were measured using 22 coaxial thermocouples. Locations of the model's heat flux transducers correspond exactly to those of HYFLEX. Heat flux is calculated from model surface temperature assuming semi-infinite one-dimensional conduction. These data are compared with flight data in terms of Stanton number ratio to avoid primary wall temperature effect. Infrared (IR) imaging was also used to measure temperature at the surface, which was coated with black paint ($\varepsilon = 0.92$).

Although errors are known to occur in measuring heat flux using this configuration of coaxial thermocouples,[12] good agreement was observed between sensors and IR images at corresponding positions on the opposite side of the symmetry plane, thereby indicating that errors in resultant ratios of Stanton number ratio are within ≈0.06, as shown in Fig. 9.

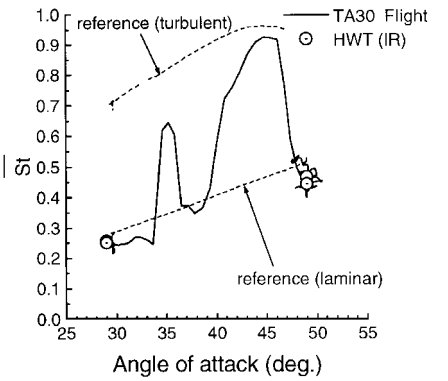

a) TA30 position

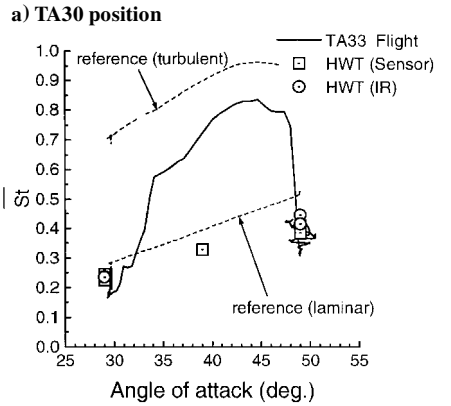

b) TA33 position

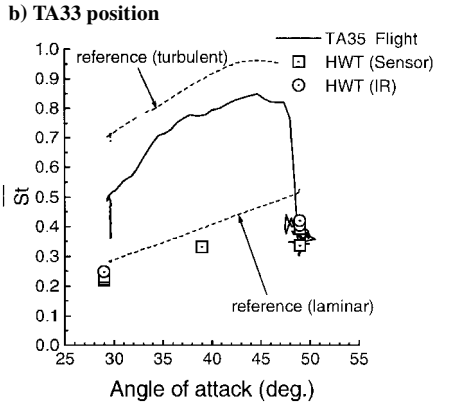

c) TA35 position

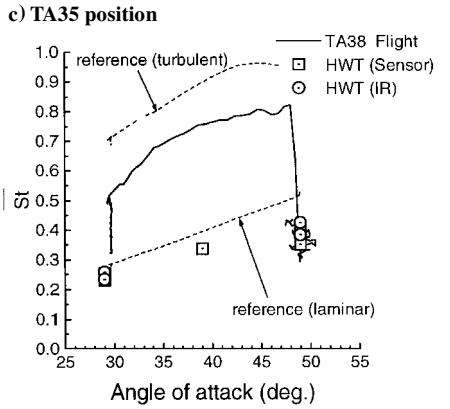

d) TA38 position

Fig. 9 Stanton number ratio vs angle of attack.

Discussion

Comparisons with Wind-Tunnel Data

We surmised that angle of attack is the predominant parameter among several affecting heating rate. This is evident when we compared Stanton number ratio vs α for flight data, wind-tunnel results, and reference values with laminar and turbulent boundary layers. Figure 9 shows the respective curves for indicated locations, where good agreement is present at each location between laminar flight data and both wind-tunnel results and laminar reference data at $\alpha = 30$ and 49 deg. Additionally, two levels in Stanton number ratio of flight data are apparent, which correspond to those with turbulent and laminar boundary layers. These results are supported by those of Fig. 6, where measured flight data of TA33 are compared to calculated results using the product of the stagnation heat transfer under the flight conditions [Eq. (1)] and the ratio of heating rate distribution from wind-tunnel results (q/q_0). With the exception of the turbulent region, good agreement is again present between the measured in-flight heating rate and the calculated results.

Boundary-Layer Transition

To analyze boundary-layer transition around HYFLEX, which has a slender body without wings, we modeled the surrounding flow as a yawed cylinder. As HYFLEX's predominant radius of curvature is 0.4 m (Fig. 10), this value was used as the radius of the yawed cylinder.

The Reynolds number based on a characteristic length scale η^* proposed by Poll[4] for attachment line transition of an infinite yawed cylinder in compressible flow can be determined from

$$\bar{R}^* = u_e \eta^* / \nu^*$$

where

$$\eta^* = \sqrt{\frac{\nu^*}{k}}, \qquad k = \frac{\mathrm{d}v_e}{\mathrm{d}y} \tag{2}$$

Local flow conditions are calculated using the entropy occurring behind the oblique shock parallel to the vehicle axis. Figure 11 shows $\bar{R}^*$ values along the flight path, as well as those determined using Poll's criteria of a critical Reynolds number with a large disturbance source upstream ($\bar{R}^* = 245$) and that without any disturbance source upstream ($\bar{R}^* = 650$). Transition is considered to occur between these values when surface roughness exceeds the critical roughness height. Although it is difficult to determine the critical roughness height due to dependence on many parameters, Murakami et al.[5] reported that under their test conditions it ranges from $0.2\eta^*$ to $1.4\eta^*$. The gaps and steps between HYFLEX tiles were controlled such that they were smaller than 1.6 and 1.0 mm, respectively. Unfortunately, however, individual gaps and steps were not measured, hence making it difficult to accurately evaluate the condition at which boundary-layer transition occurs. As a result, we assume an effective roughness height Δs of 1.0 mm.

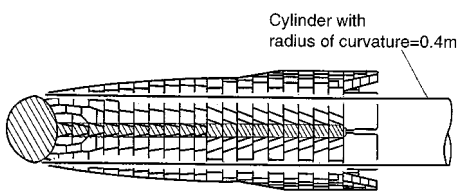

Fig. 10 Area of constant curvature along the windward surface of HYFLEX. Hatched area has constant radius of curvature (r = 0.4 m).

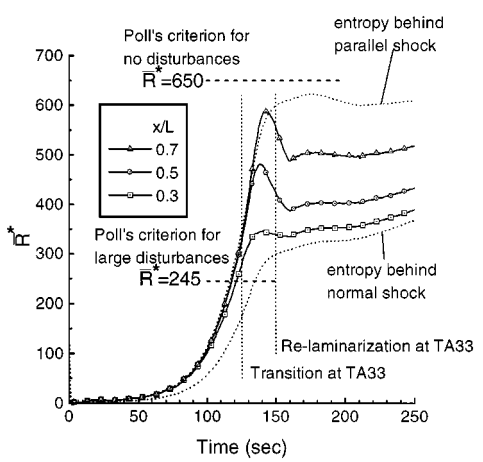

Fig. 11 Comparison of transition Reynolds number with Poll's[4] criterion.

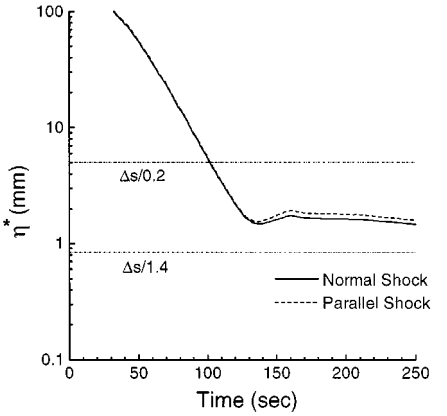

Fig. 12 Variation of the characteristic length along the HYFLEX flight path.

Figure 12 shows variations in characteristic length η^* along the flight path, where $\eta^* = \Delta s/0.2$ and $\Delta s/1.4$ are indicated. As shown, because both curves of η^* with entropy that occurs behind normal shock and oblique shock parallel to the vehicle axis are about 1.2 mm after 120 s, tile gaps/steps of HYFLEX can reach the critical roughness height for attachment line transition in the flight condition when the transition is observed. From these results, it was made clear that, by taking into account surface roughness due to tile gaps/steps, the condition at which boundary-layer transition occurs can be reasonably estimated.

Relaminarization

The occurrence of relaminarization at the windward side cannot be fully explained using $\bar{R}^*$ of an infinite yawed cylinder in which constant entropy is assumed along the streamline as the criterion because the value of $\bar{R}^*$ is nearly constant and greater than that at transition (see Fig. 11). Therefore, to account for the effect of bluntness, a mass flux balance technique was utilized under the assumption that the shape of the shock occurring in the symmetry plane is identical with that of a hyperboloid approximated using schlieren images obtained from wind-tunnel tests. Figure 11 shows the variable entropy effect on $\bar{R}^*$ at $x/L = 0.3$–0.7.

In Fig. 11, when HYFLEX took a nearly constant angle of attack of 49 deg, the variable entropy effect seems small because of rapidly diverging streamlines. On the contrary, the decrease in angle of attack at $t = 125$–150 s makes streamlines spread less, which consequently causes entropy at the boundary-layer edge to decrease toward that behind the normal shock. As a result, curves of $\bar{R}^*$ at each x/L fell off with decreasing α, a behavior that should produce relaminarization. Although $\bar{R}^*$ as indicated here may include errors caused by inaccurately estimating variable entropy effects due to the approximation of the shock shape and/or the velocity field, these results nonetheless indicate that relaminarization observed in HYFLEX is assuredly caused by the nose bluntness effect. To confirm this, however, more accurate quantitative analysis is required using local flow conditions.

Conclusion

Aerodynamic heating rates occurring near the windward centerline of HYFLEX are derived from actual surface temperature measurements in conjunction with using a newly developed thermal model of the sensor. The aerodynamic heating showed two levels, which correspond to turbulent heating and laminar heating. For a

laminar boundary layer, the heating rates in the flight show good agreement with hypersonic wind-tunnel data in terms of Stanton number ratio $\overline{St}$.

The boundary-layer transition that occurred on the windward side of HYFLEX can be explained using an attachment line transition criterion for a yawed cylinder, whose radius is identical to that of HYFLEX, in which with the roughness effect is included. Moreover, the variable entropy effect is qualitatively estimated by the axisymmetric analog technique assuming a shape of the shock in the symmetry plane. From this estimation, relaminarization of the turbulent boundary layer observed at TA21 and TA30 is considered to be caused by the effect of variable entropy.

References

[1]Zoby, E. V., Moss, J. N., and Sutton, K., "Approximate Convective-Heating Equations for Hypersonic Flows," *Journal of Spacecraft and Rockets*, Vol. 18, No. 1, 1981, pp. 64–70.

[2]DeJarnette, F. R., and Davis, R. M., "A Simplified Method for Calculating Laminar Heat Transfer over Bodies at an Angle of Attack," NASA TN-D-4720, Aug. 1968.

[3]Goodrich, W. D., Derry, S. M., and Bertin, J. J., "Shuttle Orbiter Boundary Layer Transition at Flight and Wind Tunnel Conditions," *Shuttle Performance: Lessons Learned*, Pt. 2, NASA CP-2283, 1983, pp. 753–779.

[4]Poll, D. I. A., "Transition Description and Prediction in Three-Dimensional Flows," AGARD Rept. 709, June 1984, pp. 5-1–5-23.

[5]Murakami, A., Stanewsky, E., and Krogmann, P., "Boundary-Layer Transition on Swept Cylinders at Hypersonic Speeds," *AIAA Journal*, Vol. 34, No. 4, 1996, pp. 649–654.

[6]Shirouzu, M., and Watanabe, S., "On the Hypersonic Flight Experiment (HYFLEX) for the Development of HOPE," AIAA Paper 93-5080, Nov. 1993.

[7]Shirouzu, M., Watanabe, S., and Suzuki, H., "A Quick Report of the Hypersonic Flight Experiment, HYFLEX," 20th International Symposium on Space Technology and Science, Paper 96-f-09, May 1996.

[8]Inoue, Y., Fujii, K., Takizawa, M., Takaki, R., Watanabe, S., and Ito, T., "Flight Results of HYFLEX Onboard Measurements," AIAA Paper 96-4528, Nov. 1996.

[9]Watanabe, S., Ishimoto, S., and Yamamoto, Y., "Aerodynamic Characteristics Evaluation of Hypersonic Flight Experiment Vehicle Based on Flight Data," *Journal of Spacecraft and Rockets*, Vol. 34, No. 4, 1997, pp. 464–470.

[10]Van Driest, E. R., "The Problem of Aerodynamic Heating," *Aeronautical Engineering Review*, Vol. 15, No. 10, 1956, pp. 26–41.

[11]Rakich, J. V., and Mateer, G. G., "Calculation of Metric Coefficients for Streamline Coordinates," *AIAA Journal*, Vol. 10, No. 11, 1972, pp. 1539, 1540.

[12]Kidd, C. T., Nelson, C. G., and Scott, W. T., "Extraneous Thermoelectric EMF Effects Resulting from the Press-Fit Installation of Coaxial Thermocouples in Metal Models," *Proceedings of the 40th International Instrument Symposium*, Instrument Society of America, 1994, pp. 317–335 (Paper 94-1022).

T. C. Lin
Associate Editor